

# NATURAL CONVECTION IN A RECTANGULAR ENCLOSURE DIFFERENTIALLY HEATED IN THE CORNER REGION WITH A CENTERED ADIABATIC BODY

Thiago P. Lima, thiagopl@fem.unicamp.br

Marcelo M. Ganzarolli, ganza@fem.unicamp.br

Departamento de Energia, Faculdade de Engenharia Mecânica, Universidade Estadual de Campinas, CEP 13081-860, Campinas, São Paulo, Brasil.

**Abstract.** A numerical study of the steady state natural convection in a rectangular enclosure heated from below and cooled from the side with a squared centered adiabatic body is performed in this work. The Finite Volume Method is applied using the SIMPLE algorithm to solve the phenomenon governing equations. The code is validated with results of benchmark literature. Results are discussed for Rayleigh numbers in the range of  $10^3$ - $10^6$  and Prandtl number of 0.7. The effects of the body size on the enclosure heat transfer and fluid flow are presented in terms of streamlines, isotherms, heatlines and Nusselt number. By adding an adiabatic body within the enclosure an enhancement in the heat transfer is achieved for high Rayleigh numbers.

**Keywords:** natural convection, enclosures, inner body

## 1. NOMENCLATURE

$g$	gravity acceleration	$y$	vertical coordinate
$H$	enclosure height	$W$	adiabatic block height
$N$	normal direction to a surface	<b>Greek Symbols</b>	
$Nu$	average Nusselt number	$\alpha$	thermal diffusivity
$P$	dimensionless pressure	$\zeta$	dimensionless block size
$p$	pressure	$\theta$	dimensionless temperature
$Pr$	Prandtl number, $\nu/\alpha$	$\nu$	kinematic viscosity
$Ra$	Rayleigh number, $g\beta H^3 \Delta T/\nu\alpha$	$\rho$	specific mass
$T$	temperature	$\phi$	generalized dimensionless variable
$u$	velocity in x direction	$\psi$	stream function
$U$	dimensionless velocity in x direction	$\Omega$	heat function
$v$	velocity in y direction	<b>Subscripts</b>	
$V$	dimensionless velocity in y direction	0	reference state
$X$	dimensionless x coordinate	$c$	cold wall
$x$	horizontal coordinate	$h$	hot wall
$Y$	dimensionless y coordinate	$max$	maximum

## 2. INTRODUCTION

Square enclosures have been studied by many authors (Ostrach, 1988). Its applications in engineering embrace fields as designing of buildings, solar collectors and cooling of electronic components. This fundamental class of heat transfer problem is commonly studied through two main configurations, namely, vertical and horizontal enclosures. Few works were dedicated to the study of enclosures differentially heated in the corner as well as with a centered solid body in its interior.

House *et al.* (1990) studied the effect of a centered conducting solid body of different sizes in a vertical enclosure. In the work of Oh *et al.* (1997) a heat generating solid body was placed also at the center of a vertical enclosure. Ha *et al.*

(1999) studied the transient behavior of a vertical enclosure with a heat generating solid body in its interior. In Ha et al. (2002) a horizontal enclosure within a solid body under different imposed temperatures was analyzed. Lee and Ha (2005) used a conducting body to the same enclosure. Mezrhab *et al.* (2005) added a radiation heat transfer to the problem of the vertical enclosure with a centered solid body. Except for House *et al.* (1990) the studies related above used a block of fixed size. In Bhave *et al.* (2006) the optimal size of an adiabatic centered solid body in a vertical enclosure was studied aiming the heat transfer enhancement in the enclosure. In the work Zhao *et al.* (2007) the conjugate heat transfer in a vertical enclosure with different conducting block sizes was analyzed.

The aim of this work is to study the effect of a centered adiabatic solid body in an enclosure differentially heated in the corner region. The effects of the body size are analyzed and presented in terms of streamlines, isotherms, heatlines and Nusselt number

### 3. MATHEMATICAL FORMULATION

The enclosure of the present study is filled with an incompressible Newtonian fluid with an internal centered adiabatic body. The flow is considered as steady, laminar and bidimensional. The properties are assumed constant in the conservation equations except for the buoyancy term in the momentum equation where the Boussinesq approximation is adopted. In order to give generality to the analyses performed it is convenient to write the conservation equations in their dimensionless form. Therefore, the conservation equations for the fluid region are as follows:

$$\frac{\partial U}{\partial X} + \frac{\partial V}{\partial Y} = 0 \quad (1)$$

$$U \frac{\partial U}{\partial X} + V \frac{\partial U}{\partial Y} = -\frac{\partial P}{\partial X} + Pr \left( \frac{\partial^2 U}{\partial X^2} + \frac{\partial^2 U}{\partial Y^2} \right) \quad (2)$$

$$U \frac{\partial V}{\partial X} + V \frac{\partial V}{\partial Y} = -\frac{\partial P}{\partial Y} + Pr \left( \frac{\partial^2 V}{\partial X^2} + \frac{\partial^2 V}{\partial Y^2} \right) + RaPr\theta \quad (3)$$

$$U \frac{\partial \theta}{\partial X} + V \frac{\partial \theta}{\partial Y} = \left( \frac{\partial^2 \theta}{\partial X^2} + \frac{\partial^2 \theta}{\partial Y^2} \right) \quad (4)$$

The corresponding boundary conditions are:

$$X = 0 \rightarrow U = V = 0, \quad \theta = 1 \quad (5)$$

$$X = 1 \rightarrow U = V = 0, \quad \frac{\partial \theta}{\partial X} = 0 \quad (6)$$

$$Y = 0 \rightarrow U = V = 0, \quad \theta = 0 \quad (7)$$

$$Y = 1 \rightarrow U = V = 0, \quad \frac{\partial \theta}{\partial Y} = 0 \quad (8)$$

At the body surface the boundary conditions are:

$$U = V = 0, \quad \frac{\partial \theta}{\partial N} = 0 \quad (9)$$

Where  $N$  is the direction normal to any surface of the body. The scales adopted are shown below:

$$U = \frac{uH}{\alpha}, \quad V = \frac{vH}{\alpha}, \quad X = \frac{X}{H}, \quad Y = \frac{y}{H}, \quad \theta = \frac{T - T_c}{T_h - T_c} \quad \text{and} \quad P = \frac{(p - \rho_0 g y)H^2}{\rho \alpha^2} \quad (10)$$

In order to assess the heat transfer at the vertical wall of the enclosure the averaged Nusselt number is calculated

according to Eq. (11):

$$Nu_c = - \int_0^1 \frac{\partial \theta}{\partial X} \Big|_{X=0} dY. \quad (11)$$

For purposes of visualization of the fluid flow and convective heat transfer the stream function and heat function (Kimura and Bejan, 1983) are employed in this work whose definitions in its dimensionless form are:

$$\frac{\partial \psi}{\partial Y} = U, \quad \frac{\partial \psi}{\partial X} = -V \quad (12)$$

$$\frac{\partial \Omega}{\partial Y} = U\theta - \frac{\partial \theta}{\partial X}, \quad \frac{\partial \Omega}{\partial X} = -V\theta + \frac{\partial \theta}{\partial Y} \quad (13)$$

#### 4. NUMERICAL PROCEDURE

The Finite Volume Method and the SIMPLE algorithm are used to solve numerically the phenomenon governing equations. The convective terms are discretized using the Power-law scheme whereas the central difference scheme is used for the diffusion terms discretization. The Eq. (1) to (4) are solved for the entire domain. In the solid region the coefficient of the diffusion terms of Eq. (2) and (3) is set to a high number in a way that velocity approaches zero. The solution iterative process starts from an arbitrary  $\phi$  field and the convergence criterion is reached when the Eq. (14) is satisfied.

$$\sum_{i,j} \frac{|\phi_{ij}^n - \phi_{ij}^{n+1}|}{\phi_{ij}^n} \leq \varepsilon \quad (14)$$

Where  $\phi$  represents the variables  $U$ ,  $V$  and  $\theta$ ,  $n$  is the iteration order and the value of  $\varepsilon$  chosen is  $10^{-6}$ . Variations in the  $\phi$  field for smaller values of  $\varepsilon$  shown to be insignificant.

Once the temperature and velocity fields are known, the stream and heat functions are calculated at the vertices of each control volume by integration of the Eq. (12) and (13). The singularity on the calculus of the heat flow at the intersection point of the two walls that the temperature are imposed is treated by setting the average temperature of the adjacent walls to the intersection point and by adopting a linear temperature profile between the intersection point and the first adjacent points in both walls. See Ganzarolli and Milanez (1995) for a wider discussion.

In order to validate the code the results generated by the present study were compared with results of the literature on vertical enclosures (de Vahl Davis, 1983) without and with the inner body (House *et al.*, 1990) showing a good agreement. After a grid refinement study the grid size chosen was of 160x160 volumes based on the relative error of the maximum stream function calculated.

#### 5. RESULTS AND DISCUSSION

In this section the results obtained according to the methodology described in the last section are presented and discussed.

##### 5.1 Velocity and temperature fields

In the figures showing isolines nine lines are plotted forming ten equally spaced intervals between the minimum and maximum values of stream function, temperature and heat function.

Figure (1) shows the streamlines, isotherms and heatlines of the enclosure studied without the block for  $Pr=0.7$  and  $Ra=10^3-10^6$ . For the enclosure without the block the inner flow occurs in a counterclockwise single cell. For high Rayleigh numbers this pattern can be qualitatively approximated to four jets connected at the enclosure vertices circulating around a low velocity region as proposed in Ganzarolli (1991, p. 60).

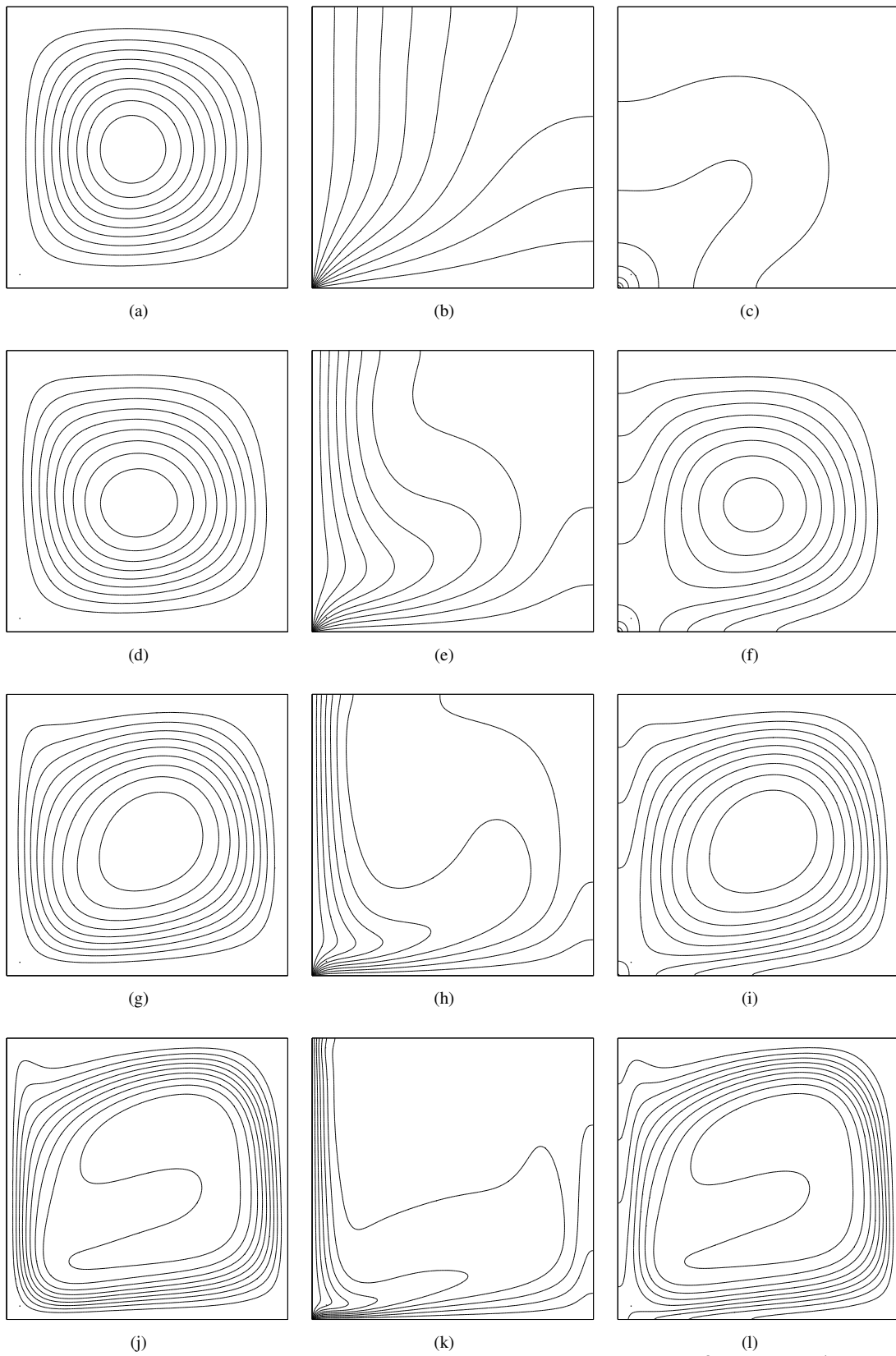


Figure 1. Streamlines (left), isotherms (center) and heatlines (right) for  $Pr=0.7$  and  $Ra=10^3$  (a, b, c),  $10^4$  (d, e, f),  $10^5$  (g, h, i) and  $10^6$  (j, k, l)

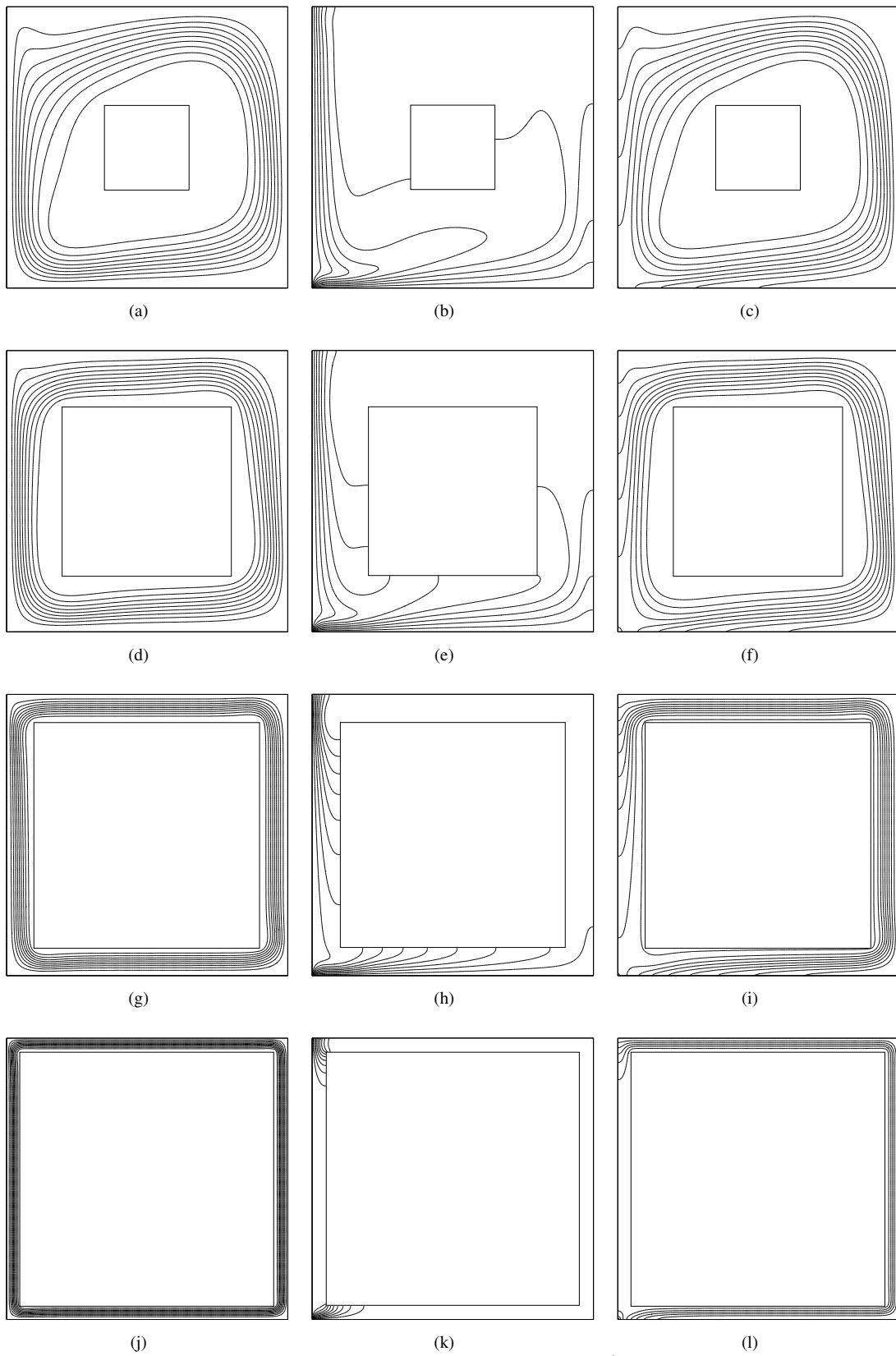


Figure 2. Streamlines (left), isotherms (center) and heatlines (right) for  $Ra=10^6$ ,  $Pr=0.7$  and  $\zeta=0.3$  (a, b, c),  $\zeta=0.6$  (d, e, f),  $\zeta=0.8$  (g, h, i) and  $\zeta=0.9$  (j, k, l)

Figure (2) shows the streamlines, isotherms and heatlines of the enclosure studied for Rayleigh and Prandtl numbers of  $10^6$  and 0.7, respectively, and dimensionless block size defined as  $\zeta=W/H$  equal to 0.3, 0.6, 0.8 and 0.9. In the isolines shown in Fig. (2a) and (2b) the adiabatic block shows little influence on the velocity and temperature fields of the enclosure that maintains the same characteristics of the fields of the enclosure without the block (Fig. (1a) and (1b)). For high Rayleigh numbers the core of the enclosure without the block remains relatively stagnated. This core grows with the increase of the Rayleigh number as predicted by the scale analysis presented in Bejan (1995, p. 223) for a vertical enclosure and also applied in Ganzarolli and Milanez (1995) for an enclosure with boundary conditions similar to the ones presented in this work. For  $Ra=10^3$  (Fig. (1a)) and  $Ra=10^6$  (Fig. (1j)) this core has roughly the dimensions of  $\zeta=0.1$  and 0.5, respectively, considering for that the region enclosed by the streamline  $\psi=0.9\psi_{max}$ . Therefore the increase of the block up to approximately the size of this core slightly alters the velocity and temperature fields of the enclosure.

In Fig. (2) the pattern with the four jets is maintained now due to a geometrical obstruction. For  $\zeta=0.6$  (Fig. (2d)) the flow begins to assume the pattern also seen in loops (Ramos *et al.*, 1990) but slightly rotated in the flow direction, with the streamlines concentrated on the center of the channels. The upper horizontal channel discharges fluid on the cold wall (Fig. (2e)) with the same temperature profile of the upper wall jet for the enclosure without the block (Fig. (1k)). With further increase of the block this temperature profile rises in comparison with the upper wall jet of the enclosure without the block.

From a block size of  $\zeta=0.8$  (Fig. (2h)) the fluid heated on the hot wall begins to flow through the right channel almost isothermally, rising and reaching the cold wall in the same fashion. Up to this point the heat transfer within the enclosure still occurs through the whole extent of the two fixed temperature walls, being the energy flow more concentrated on the left half and upper half of the hot and cold wall, respectively (Fig. (2i)). With the value of  $\zeta=0.9$  (Fig. (2k)) the temperature field shows some alterations. In this new pattern the fluid circulates around three thirds of the enclosure almost isothermally and the major part of the heat transfer is restricted to a short extent at the entrance and exit of the cold wall, upper and bottom left corner of the enclosure, respectively (Fig. (2l)).

As the channels narrow the convective flow becomes weaker and the heat transfer concentrates at the entrance of the hot and cold wall. The decrease of the flow can be seen through the abrupt decrease of the maximum stream function value from  $\phi_{max}=11.6$  ( $\zeta=0.8$ ) to  $\phi_{max}=2.6$  ( $\zeta=0.9$ ) for  $Ra=10^6$ . Due to the weaknesses of the flow, diffusion becomes dominant in the heat transfer within the enclosure and a considerable part of the heat leaves the hot wall towards the cold wall without to circulate around the block (Fig. (2l)). A similar pattern is found in House *et al.* (1990) for a vertical enclosure with a conducting block, but differently, that pattern was attributed to the heat transfer through the corner of the block from the fluid at the entrance of the hot (cold) wall and the fluid arriving at the same wall. For low Rayleigh numbers, this pattern is observed for smaller block sizes. For  $Ra=10^3$  and  $\zeta=0.5$  none of the heatlines circulates the block, forming mostly quarters of circle centered at the at bottom left vertex of the enclosure exhibiting a pattern of a quasi purely diffusive heat transfer.

## 5.2 Heat transfer

The last section presented some aspects regarding the influence of the block in the temperature and velocity fields of the enclosure. The implications of these alterations on the heat transfer of the enclosure will be discussed in this section. Figure (3) shows the variation of the Nusselt number as a function of the block size for different Rayleigh numbers.

As shown in Fig. (1) with the increasing of Rayleigh number the convective heat transfer within the enclosure becomes more important. As an effect of this, the heatlines that leave the hot wall cluster in the regions of higher velocities close to walls indicating a larger energy flow in these regions. Therefore the increase of the block in the center of the enclosure causes no sensible effects on its heat transfer as far as the body boundaries reach the passages of large energy flow. This behavior is shown in Fig. (3) where for  $Ra>10^4$  the Nusselt number shows none or little variations for a block size up to  $\zeta=0.5$ . The continuous increase of the block causes an increase of the Nusselt number which reaches a maximum for distinct block sizes depending on the Rayleigh number. The higher is the Rayleigh number the larger is the block size

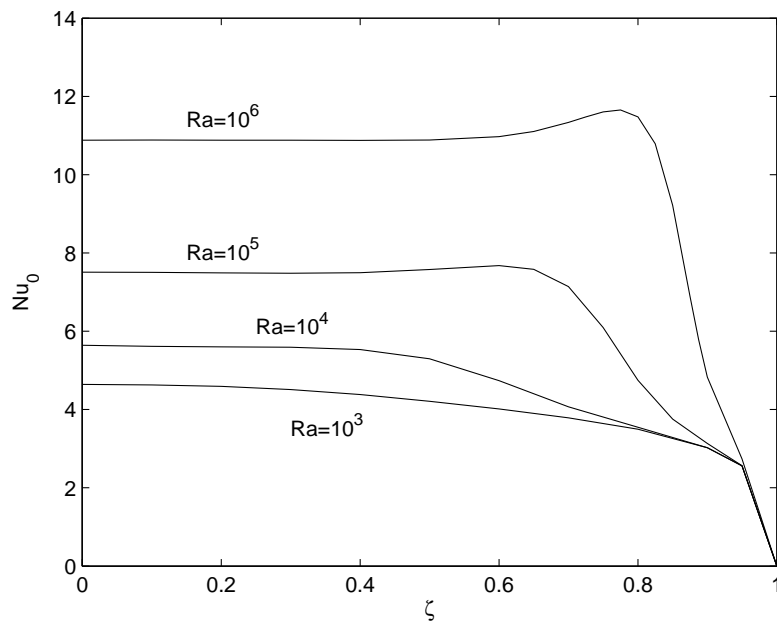


Figure 3. Variation of averaged Nusselt number as a function of dimensionless block size

where the Nusselt number reaches its maximum.

Still in this Rayleigh number range, the increase of the Nusselt number coincides with the reduction in the number of heatlines that compose the vortices in the core of the enclosure. See Fig. (2f) and (2i) compared with values of Nusselt number for  $Ra=10^6$  in Fig. (3). The increase of the block suppress the heat transfer at the enclosure core leading to a larger amount of energy that is carried by the convective flow leaving the hot wall towards the cold wall. This increase is advantageous as far as the block begins to affect the fluid flow causing an abrupt decrease of the maximum stream function as mentioned in the last section.

From this point on, the heat diffusion plays the major role on the enclosure heat transfer and the pattern shown in Fig. (2l) takes place. The heat transfer is restricted mostly at the bottom left corner of the enclosure. At this stage the magnitude of the Nusselt number approximates the levels of  $Ra=10^3$  when the heat transfer in the enclosure is almost purely diffusive (Fig. (1a), (1b) and (1c)).

For low Rayleigh numbers, the variation of the Nusselt number shows no maximum values. The heat transfer decreases continuously until the limit of zero when the block occupies the entire enclosure. For  $Ra=10^3$  the heatlines are not concentrated near the walls and no vortex is formed in the enclosure core. The increase of the block affects little the heat transfer until a block size of approximately  $\zeta=0.9$ . The reason comes from the fact that the majority of the energy that flows from the hot to cold wall is restricted to the bottom left corner of the enclosure (Fig. (1c)), which is not affected by smaller block sizes.

For  $Ra=10^4$ , although the heatlines present a vortex at the enclosure core, the convective flow is still weak and it is not concentrated near the wall as shown by the spacing of the heatlines in Fig. (1f). The majority of the energy flow still occurs by diffusion at the bottom left corner where the heatlines form a quarter of circle connecting the two adjacent walls. The Nusselt number shows a behavior similar to that of  $Ra=10^3$ . It shows no maximum value, decreasing slightly until  $\zeta=0.4$  and then more intensely until it reaches the zero limit.

## 6. CONCLUSIONS

Adding an adiabatic square block in the enclosure center enhances its internal heat transfer for Rayleigh numbers higher than  $10^4$ . This enhancement has a maximum for different block sizes depending on the Rayleigh number. The

higher is the Rayleigh number the larger is the block size where the Nusselt number reaches its maximum.

For low Rayleigh numbers the heat transfer within the enclosure occurs mainly by diffusion concentrated on the bottom left region of the enclosure. The presence of the adiabatic block leads to a continuously decrease in its heat transfer.

## 7. ACKNOWLEDGEMENTS

The authors would like to acknowledge the financial support received from the Coordenação de Aperfeiçoamento de Pessoal de Nível Superior (Capes).

## 8. REFERENCES

- Bejan, A., 1995. *Convection heat transfer*. John Wiley & Sons, 2nd edition.
- Bhave, P., Narasimhan, A. and Rees, D., 2006. "Natural convection heat transfer enhancement using adiabatic block: Optimal block size and prandtl number effect". *International Journal of Heat and Mass Transfer*, Vol. 49, pp. 3807–3818.
- de Vahl Davis, G., 1983. "Natural convection of air in a square cavity: a bench mark numerical solution". *International Journal for Numerical Methods in Fluids*, Vol. 3, No. 3, pp. 249–264.
- Ganzarolli, M.M. and Milanez, L.F., 1995. "Natural convection in rectangular enclosures heated from below and symmetrically cooled from the sides". *International Journal of Heat and Mass Transfer*, Vol. 49, pp. 1063–1073.
- Ganzarolli, M.M., 1991. *Convecção natural em cavidade retangular aquecida pela base e simetricamente resfriada pelos lados*. Ph.D. thesis, Universidade Estadual de Campinas, Campinas, SP, Brazil.
- Ha, M., Jung, M. and Kim, Y., 1999. "Numerical study on transient heat transfer and fluid flow of natural convection in an enclosure with a heat-generating conducting body". *Numerical Heat Transfer; Part A: Applications*, Vol. 35, No. 4, pp. 415–433.
- House, J.M., Beckermann, C. and Smith, T.F., 1990. "Effect of a centered conducting body on natural convection heat transfer in an enclosure". *Numerical Heat Transfer; Part A: Applications*, Vol. 18, No. 2, pp. 213–225.
- Kimura, S. and Bejan, A., 1983. "The heatline visualization of convective heat transfer". *ASME Journal of Heat Transfer*, Vol. 105, pp. 916–919.
- Lee, J.R. and Ha, M.Y., 2005. "Numerical study of natural convection in a horizontal enclosure with a conducting body". *International Journal of Heat and Mass Transfer*, Vol. 48, pp. 3308–3318.
- Mezrhab, A., Bouali, H., Amaoui, H. and Bouzidi, M., 2005. "Computation of combined natural-convection and radiation heat-transfer in a cavity having a square body at its center". *Applied Energy*, Vol. 83, pp. 1004–1023.
- Oh, J., Ha, M. and Kim, K., 1997. "Numerical study of heat transfer and flow of natural convection in an enclosure with a heat-generating conducting body". *Numerical Heat Transfer Part A: Applications*, Vol. 31, No. 3, pp. 289–303.
- Ostrach, S., 1988. "Natural convection in enclosures". *Advances in Heat Transfer*, Vol. 8, No. 11, pp. 161–227.
- Ramos, E., Castrejón, A. and Gordon, M., 1990. "Natural convection in a two-dimensional square loop". *International Journal of Heat and Mass Transfer*, Vol. 33, No. 5, pp. 917–930.
- Zhao, F.Y., Liu, D. and Tang, G.F., 2007. "Conjugate heat transfer in square enclosures". *Heat Mass Transfer*, Vol. 43, No. 9, pp. 907–922.

## 9. RESPONSIBILITY NOTICE

The authors are the only responsible for the printed material included in this paper.